Research Article

OPTIMIZATION OF POTASSIUM NITRATE BASED SOLID PROPELLANT GRAINS FORMULATION USING RESPONSE SURFACE METHODOLOGY

Oladipupo Olaosebikan Ogunleye[1], Jimoh Olugbenga Hammed[2], Solomon Oluyemi Alagbe[3]

[1] Ladoke Akintola University of Technology, Nigeria, e-mail: ooogunleye@yahoo.com

[2] Center for Space Transport and Propulsion, National Space Research and Development Agency, Epe, PMB 1001, Lagos, Nigeria, e-mail: hamedjimoh45@yahoo.com

[3] Department of Chemical Engineering, Faculty of Engineering and Technology, Ladoke Akintola University of Technology, P.M.B. 4000, Ogbomoso, Nigeria, e-mail: alagbeuk@yahoo.co.uk

ABSTRACT

This study was designed to evaluate the effect of propellant formulation and geometry on the solid propellant grains internal ballistic performance using core, bates, rod and tubular and end-burn geometries. Response Surface Methodology (RSM) was used to analyze and optimize the effect of sucrose, potassium nitrate and carbon on the chamber pressure, temperature, thrust and specific impulse of the solid propellant grains through Central Composite Design (CCD) of the experiment. An increase in potassium nitrate increased the specific impulse while an increase in sucrose and carbon decreased specific impulse. The coefficient of determination (R^2) for models of chamber pressure, temperature, thrust and specific impulse in terms of composition and geometry were 0.9737, 0.9984, 0.9745 and 0.9589, respectively. The optimum specific impulse of 127.89 s, pressure (462201 Pa), temperature (1618.3 K) and thrust (834.83 N) were obtained using 0.584 kg of sucrose, 1.364 kg of potassium nitrate and 0.052 kg of carbon as well as bate geometry. There was no significant difference between the calculated and experimented ballistic properties at $p < 0.05$. The bate grain geometry is more efficient for minimizing the oscillatory pressure in the combustion chamber.

Keywords: propellant grains, specific impulse, grains performance, combustion instability, geometry.

INTRODUCTION

Solid Rocket Motor (SRM) comprises of a combustion chamber, nozzle, and grain [1]. A complex interrelationship between these three sub-systems and their proper integration determine the performance of a particular SRM mission [2]. Effort to minimize the pressure and friction losses of internal and external flows may increase the range or payload capacity of SRM. Performance characteristics, envelope constraints and mission profile are important considerations in combustion chamber design and these are hinged on grain design and burning surface of the propellant grains [3].

The nozzle is another important component of rockets because its efficiency significantly affects rocket's performance. By minimizing the losses in the nozzle, the thrust of a rocket can be increased by keeping the grain geometry fixed [3]. Specification of limiting conditions is another challenging task for a designer to prevent failures from excessive deformation of the propellant; over pressurization due to propellant cracking; casing burn-through due to premature exposure of the insulation because of the grain structural failure or the propellant-insulation-motor casing bond failure [4].

Standard composite propellants for space applications contain metal powders for the increment of gravimetric specific impulse. The final formulation is usually a compromise between 10–14% of binder, 60–80% of oxidizer

and up to 20% of metal [5, 6]. When metalized propellants burn, a complex process of aggregation to agglomeration takes place at the burning surface. Condensed combustion products that leave the burning surface are released in the gas phase where combustion process keeps progressing while they move towards the nozzle [7]. The rocket motor's operation in terms of volumetric efficiency and average pressure over the course of the burn depends combustion characteristics of the propellants, its burning rates, burning surface and grain geometry [4, 8, 9, 10].

In the modern solid propellants, the oxidant is usually one of the inorganic salts such as potassium nitrate, chlorates and perchlorates and the fuels sometimes include sulphur while carbon serves as the organic binder. The various combinations of propellants ingredients are meant to give burning stability and storage stability. The presence of carbon and the byproducts of inorganic oxidants, potassium and sodium salts produces a higher molecular weight and hence lower exhaust velocity. This affects the performance of the nozzle in converting heat energy into gas flow [11]. The overall thrust profile can be controlled by the shape of the grains as well as the stability of the thrust. The stability of the thrust is determined by the rate at which the surface of the burning grain is consumed which itself is a function of pressure in the combustion chamber. Therefore, the pressure and thrust are dependent on the recession rate and the area of the burning surface [8, 11].

Propellant grains, based on their combustion surfaces, can be classified as regressive, neutral and progressive burning. If there is a central core, it is usually a neutral burning grain; cylindrical, spherical and cubical grains exhibit regressive burning. And, multi-perforated grains are usually progressive burning [8, 12]. Temperature and pressure of the combustion chamber as well as solid propellant compositions are also important parameters affecting the burn rate [9]. Also, as initial temperature and pressure of the combustion chamber increased, the burn rate increased. With that, as the fuel temperature increased, the end pressure also increased which shortened the combustion duration [13]. Other studies whose burn rate, combustion surface and pressure relations have been investigated in a wide range of pressures includes Meda *et al.* [14], Song *et al.*[15] and found that burn rate increased not only by increasing pressure but also combustion surface area.

Many approaches, starting from gradient methods to basic heuristics, especially tailored meta-heuristics and hybrid heuristics, have been used for design and optimization process of SRM system parameters and sub-components. Design and optimization of SRM have evolved from several previous studies [16 – 28]. However, there is a need to improve SRM modelling and the application of optimization technique to relate various factors like geometries and composition to the performance of the SRM. Present research effort proposes a solution strategy using Response Surface Methodology (RSM) [29] in trying to improve the design process considering both modelling and optimization issues. The solid propellant grains considered for this study are hollow-cylindrical, bates, rod and tubular and end burn grains. Response surface methodology (RSM) has been shown to be an effective tool for optimizing a process as highlighted by various authors [29, 30].

MATERIALS AND METHODS

Propellant preparation

A solid propellant of potassium nitrate base was prepared by re-crystallization method. The basic ingredients of the solid propellant used were Sucrose, Potassium Nitrate and Carbon. The Sucrose serves as the fuel, Potassium Nitrate as the oxidizer and Carbon as a pacifier. The proportion of Sucrose in a formulation ranged between 25.6% and 38.4%, Potassium Nitrate ranged between 52% and 78% and Carbon ranged between 2.4% and 3.6%. The propellant grain of mass 2 kg was considered for the firing test of each of the formulation. The Potassium Nitrate was dissolved in hot water at 100^0C in a thermostatic bath at a ratio 1: 1 on weight to volume basis. Then the Sucrose was added at the same temperature and stirred until homogeneity was achieved. This was followed by carbon until homogeneous slurry was achieved. This slurry was then casted in an already prepared mould of hollow core, bates, rod and tubular, and end burn geometry grains. These were allowed to cure at room temperature in a desiccant for 12 hours to attain its original temperature, 298 K [Robert, 2009]. The cured propellant was removed from the mould and therefore set for combustion.

Static firing test

The prepared propellant was inserted into the combustion chamber of the De Laval nozzle SRM where it was ignited. The combustion process produced the energy that was converted to the thrust propelling the rocket to predetermined altitude. The ballistic states of the combustion process measured were pressures (MPa), temperature (K), thrust (N) and specific impulse using data acquisition system connected with rocket motor chamber. The specific impulse, I_{SP} is the thrust per unit weight flow rate of the propellant expressed as shown on equation (1). The static firing tests were carried out for combustion process at the Centre for Space Transport and Propulsion, Epe, Lagos.

$$I_{sp} = F/w \qquad (1)$$

Experimental design

In this study Central Composite Design (CCD) in RSM using Design expert software was used to design and optimise the experiment. The design was based on the fact that each of the chamber pressure, temperature, thrust and specific impulse of the SRM is functionally related to specific propellant formulation and geometry. Multiple regression equation describing ballistic properties in terms of composition and geometry were fitted. List of ingredients in the descending order of assumed importance as a propellant composition are as presented on Table 1. The composition of propellant has the following form: A (Sucrose) + B (Potassium Nitrate) + C (Carbon) = 100%. This equation implies mathematical linear dependence of the variables if the amounts of ingredients are used directly as variables, from the equation, the quantity of any ingredient is uniquely determined by the amounts of the other two. To function in a multiple factor analysis, these ingredients were transformed into ratios, which can be varied independently for mathematical consistency. For this experiment, the ingredients ratios were selected as the x_i variables as shown on equation (2) – (3):

$$x_1 = A/(B+C) = 0.471 \qquad (2)$$
$$x_2 = B/C = 21.667 \qquad (3)$$

A centre point for the design was selected with ingredients at levels expected to yield, at least, satisfactory experimental results. With the centre composition selected, the normal x_i ratios were calculated by using the normal weight composition of the formulation given in Table 1. The de-

Table 1. Propellant formulation at the design centre point

Ingredients	Centre point
A. Sucrose as fuel	32
B. Potassium nitrate as oxidizer	65
C. Carbon as opacifier	3
Total	100

sign depended upon the symmetrical selection of variation increments about the centre composition. These levels of variation were chosen to be within the range of formulation, and the increments were carefully selected, as interpretation of the result valid only within the experimental limits. The increments of variation for each variable spaced around the centre point ratios, along with the equations relating the actual and coded ratios, are presented in Table 2. By substituting these equations, compositions were coded for solution of the multiple regression equations. The coded level equations are as shown in equations (4) – (5).

Table 2. Experimental values for the experimental design

Ingredients		X_i coded levels		
(x_i)	±Increment	-1	0	1
x_1	±0.2	0.377	0.471	0.565
x_2	±0.2	17.334	21.667	26.000

Where x_i and coded X_i ratios are related by the following equations:

$$X_1 = \frac{(x_1 - 0.471)}{0.2} \qquad (4)$$
$$X_2 = \frac{(x_2 - 21.667)}{0.2} \qquad (5)$$

Before this type of experiment could be carried out, the coded X_i ratios for each formulation as per experimental design were translated into workable propellant formulation. The propellant ingredient compositions were obtained by systematic algebraic solutions for A, B and C in terms of actual x_i ratios and a unit quantity of a propellant. The resulting design is as presented in Table 3. The equations derived for the general case are equations (6) – (8). The CCD experiment used was a three factors comprising two numerical factors (X_1 and X_2) at three levels and one categorical factor (grain geometry – X_3) at four ordinal levels: core (1), bates (2), rod (3) and end burns(4) with four responses (Chamber pressure, temperature, thrust and specific impulse). X_3 was transformed

Table 3. Central composite design arrangement for propellant formulation

Runs	Coded levels of factors			Compositons (% mass)		
	X_1	X_2	Geometry	A	B	C
1	-1.000	1.000	2	0.548	1.399	0.054
2	0.000	-1.000	4	0.640	1.286	0.074
3	0.000	0.000	1	0.640	1.300	0.060
4	0.000	-1.000	3	0.640	1.286	0.074
5	1.000	1.000	1	0.722	1.231	0.047
6	-1.000	1.000	1	0.548	1.399	0.054
7	0.000	-1.000	2	0.640	1.286	0.074
8	1.000	0.000	2	0.722	1.222	0.056
9	0.000	1.000	3	0.640	1.309	0.050
10	-1.000	-1.000	3	0.548	1.373	0.079
11	-1.000	0.000	1	0.548	1.388	0.064
12	1.000	1.000	2	0.722	1.231	0.047
13	0.000	1.000	2	0.640	1.309	0.050
14	1.000	0.000	4	0.722	1.222	0.056
15	1.000	1.000	4	0.722	1.231	0.047
16	0.000	0.000	2	0.640	1.300	0.060
17	1.000	1.000	3	0.722	1.231	0.047
18	-1.000	1.000	3	0.548	1.399	0.054
19	0.000	1.000	4	0.640	1.309	0.050
20	0.000	-1.000	1	0.640	1.286	0.074
21	-1.000	-1.000	2	0.548	1.373	0.079
22	-1.000	0.000	4	0.548	1.388	0.064
23	1.000	-1.000	3	0.722	1.208	0.070
24	1.000	0.000	1	0.722	1.222	0.056
25	0.000	0.000	4	0.640	1.300	0.060
26	1.000	0.000	3	0.722	1.222	0.056
27	0.000	0.000	3	0.640	1.300	0.060
28	1.000	-1.000	2	0.722	1.208	0.070
29	0.000	1.000	1	0.640	1.309	0.050
30	-1.000	-1.000	1	0.548	1.373	0.079
31	-1.000	0.000	2	0.548	1.388	0.064
32	-1.000	1.000	4	0.548	1.399	0.054
33	1.000	-1.000	1	0.722	1.208	0.070
34	-1.000	0.000	3	0.548	1.388	0.064
35	-1.000	-1.000	4	0.548	1.373	0.079
36	1.000	-1.000	4	0.722	1.208	0.070

to ordinal categorical variable for ease of mathematical analysis. The resulting weights for each ingredient in different propellant formulation are as presented in Table 3.

$$A = \frac{x_1}{1 + x_1} \quad (6)$$

$$B = \frac{x_2(1 - A)}{1 + x_2} \quad (7)$$

$$C = \frac{1 - A}{1 + x_2} \quad (8)$$

Data analysis and optimization

Multiple regression analysis was used to fit the model represented by equation (9) to the experimental data. In order to analyze the experimental design by RSM, it was assumed that there existed a mathematical function, f_h ($h = 1, 2, ..., n$) for each response variable, Y_h in term of m independent ballistic variable X_i ($i = 1, 2, ..., n$).

$$Y_h = f_h(X_2, X_2, ..., X_n) \quad (9)$$

In this experiment, $n = 2$ and $m = 4$. In order to approximate this function a second order polynomial equation (10) was assumed.

$$Y_h = b_{h_o} + \sum_{i=1}^{m} b_{h_i} X_i + \sum_{i=1}^{m} b_{h_i} X^2_i + \sum_{i \neq j=1}^{m} b_{h_j} X_i X_j \quad (10)$$

Where b_{h_o} is the value of fitted response at the centre point of the design, i.e. (0, 0) and b_{h_i}, $b_{h_{ii}}$ and b_{ij} are linear, quadratic and cross product regression term respectively.

Maximization and minimization of the polynomial thus fitted was performed by numerical techniques, using the mathematical optimizer procedure of Design Expert 6.8 that deals with constraints. The constraints are set to get the coded value of a variable between the lower and upper limits for an optimum response (a minimum and a maximum level must be provided for each parameter included). The response surfaces and perturbation plots for these models were plotted as a function of two variables, while keeping the other variables at the optimum level.

RESULTS AND DISCUSSION

Effects of propellant formulation and geometry on ballistic properties.

The effects of various propellant formulation and geometry on the internal ballistic properties of the SRM as obtained from static firing tests are as presented in Table 4. Considering the four geometries studied, chamber pressure, chamber temperature, thrust and specific impulse decreased with increasing sucrose while they all increased with increasing potassium nitrate. However, as pointed out by Sutton and Biblarz, [8] and Turner [11] and, the fundamental requirement of a SRM is to develop very high thrust per mass. This then shows the importance of the specific impulse in the discussion of the SRM performance and that since the effect of the other three are directly linked to it, its trend can simply be used to explain that of others. The general increment of specific impulse with the increase in potassium nitrate is due to the presence of more oxidizer to improve the efficiency of combustion in the chamber thereby increasing the conversion of heat energy to thrust and reducing the weight of the particles that are byproducts of combustion. This finding is in line with the result of Wu *et al.* [13] and Richards [31]. Bates grains had the highest specific impulse within the range of

solid propellant formulations verified with the firing static test. The bates grains burnt within 3 s with maximum specific impulse of 127.9 s when compared with other grains considered such as Hollow-Cylindrical core grains that also burnt in 3.5 s but with the specific impulse of 80.6s, Rod and Tubular burnt in 4 s with specific impulse of 86.9 s and End Burn grains burnt in 5 s with specific impulse of 85.6 s. The best specific impulse was achieved in bates grains because much more surface area was exposed to burning which actually accounted for its lowest burn time compared with other grains geometry. This is in agreement with some previous works [4, 8, 9, 10, 32]. The perturbation graph of the four geometries showing the variation of specific impulse with varying propellant compositions are as shown on Figure 1. From this observation, as more surface area is being exposed to burning, there will be corresponding increase in specific impulse and by implication thrust of a propellant. This will automatically reduce the pressure, increase burn rate, reduce erroneous burning and enhanced the combustion stability of the SRM.

Estimation of the fitted models parameters

In developing the mathematical models for ballistic internal properties (chamber pressure, chamber temperature, thrust and specific impulse) of the solid propellant, multiple regression analyses were conducted in obtaining the models. All main effects, linear and quadratic, and interaction were estimated for each model. The coefficients of each factor as well as the coefficient of determination obtained for each model are as presented on Table 5. The square of the coefficients of regression (R^2) for chamber pressure, chamber temperature, thrust and specific impulse models are 0.9737, 0.9984, 0.9745 and 0.9589, respectively. These values are quite high for response surfaces and indicated that the fitted quadratic models accounted for more than 98% of the variance in the experimental data. In estimating these models, the categorical factor (geometry) has been coded numerically by the software in order to accommodate the variation of geometries in the final analysis of the model. Ordinal categorical factor can used when the ordering can be interpreted with meaning and the treatments are numeric. If there is no "number" that makes sense, a numeric rank can be used and this has been adopted in this study. Based on t-statistics,

Table 4. Effects of the propellant formulation on ballistic properties

Runs	Coded factors			Actual weight of ingredients(kg)			Responses			
	X_1	X_2	Geometry	A	B	C	P(Pa)	T(K)	F(N)	I_{sp}(s)
1	-1.000	1.000	2	0.548	1.399	0.054	462201	1655.2	835.6	127.9
2	0.000	-1.000	4	0.640	1.286	0.074	139801	1436.6	252.7	64.5
3	0.000	0.000	1	0.640	1.300	0.060	276616	1502.8	500.1	75.5
4	0.000	-1.000	3	0.640	1.286	0.074	201037	1454.4	363.4	74.2
5	1.000	1.000	1	0.722	1.231	0.047	271192	1411.2	490.3	75
6	-1.000	1.000	1	0.548	1.399	0.054	300990	1617.6	526.4	80.6
7	0.000	-1.000	2	0.640	1.286	0.074	304668	1473	550.8	84.3
8	1.000	0.000	2	0.722	1.222	0.056	181021	1374.1	327.2	50.1
9	0.000	1.000	3	0.640	1.309	0.050	232517	1514.5	420.3	85.8
10	-1.000	-1.000	3	0.548	1.373	0.079	223961	1555.6	404.9	82.6
11	-1.000	0.000	1	0.548	1.388	0.064	290095	1590.5	524.4	80.3
12	1.000	1.000	2	0.722	1.231	0.047	245259	1408.9	443.4	67.9
13	0.000	1.000	2	0.640	1.309	0.050	432085	1550.3	781.1	119.6
14	1.000	0.000	4	0.722	1.222	0.056	106236	1357.8	192.1	49
15	1.000	1.000	4	0.722	1.231	0.047	134984	1389.5	244	62.3
16	0.000	0.000	2	0.640	1.300	0.060	356742	1516.5	644.9	98.7
17	1.000	1.000	3	0.722	1.231	0.047	203088	1403.3	367.1	74.9
18	-1.000	1.000	3	0.548	1.399	0.054	237264	1602.9	428.9	87.5
19	0.000	1.000	4	0.640	1.309	0.050	179088	1498.4	323.8	82.6
20	0.000	-1.000	1	0.640	1.286	0.074	262273	1466.6	474.1	72.6
21	-1.000	-1.000	2	0.548	1.373	0.079	399655	1594.9	722.5	110.6
22	-1.000	0.000	4	0.548	1.388	0.064	180839	1554.9	326.9	83.4
23	1.000	-1.000	3	0.722	1.208	0.070	167110	1323.1	302.1	61.6
24	1.000	0.000	1	0.722	1.222	0.056	254818	1382.7	460.7	70.5
25	0.000	0.000	4	0.640	1.300	0.060	161873	1472.5	292.6	74.7
26	1.000	0.000	3	0.722	1.222	0.056	180527	1374.1	326.4	66.6
27	0.000	0.000	3	0.640	1.300	0.060	219245	1490.8	396.3	80.9
28	1.000	-1.000	2	0.722	1.208	0.070	115474	1316.4	208.8	31.9
29	0.000	1.000	1	0.640	1.309	0.050	285945	1525.6	516.9	79.1
30	-1.000	-1.000	1	0.548	1.373	0.079	282652	1570.8	511	78.2
31	-1.000	0.000	2	0.548	1.388	0.064	453120	1623.9	819.1	125.4
32	-1.000	1.000	4	0.548	1.399	0.054	185538	1582.2	335.4	85.6
33	1.000	-1.000	1	0.722	1.208	0.070	233846	1327.4	422.7	64.7
34	-1.000	0.000	3	0.548	1.388	0.064	235467	1574.8	425.7	86.9
35	-1.000	-1.000	4	0.548	1.373	0.079	165269	1533.2	298.8	76.2
36	1.000	-1.000	4	0.722	1.208	0.070	100373	1313.9	181.5	46.3

the regression coefficients that are not significant at 95% were discarded while only those that are significant were selected for the models of chamber pressure, chamber temperature, thrust and specific impulse as shown in equations (11) – (14)

$$P = 2.551E + 005 - 50963.46\,X_1 + 23918.00\,X_2 +$$
$$32523.31X_3[1] + 87167.53X_3[2] - 29500.14\,X_3[3] +$$
$$31983.29X_1X_3[1] - 77906.87\,X_1X_3[2] +$$
$$26635.63X_1X_3[3] - 10692.00X_2X_3[1] +$$
$$29373.33X_2X_3[2] - 10457.83X_2X_3[3] - 20533.37X_1^2$$
$$(11)$$

$$T = 1494.76 - 111.42X_1 + 33.07X_2 +$$
$$6.66\,X_3[1] + 19.78X_3[2] - 4.64\,X_3[3] +$$
$$8.04X_1X_2 + 1.82\,X_1X_3[1] - 17.68X_1X_3[2]$$
$$+ 5.95X_1X_3[3] - 1.47X_2X_3[1] + 5.28X_2X_3[2] -$$
$$1.80X_2X_3[3] - 15.21X_1^2 - 4.39X_2^2 \qquad (12)$$

$$F = 461.59 - 91.39\,X_1 + 42.50\,X_2 + 57.32\,X_3[1] +$$
$$158.08\,X_3[2] - 52.85\,X_3[3] + 60.04\,X_1X_3[1] -$$
$$141.58\,X_1X_3[2] + 47.40\,X_1X_3[3] - 21.53X_2X_3[1]$$
$$+ 53.84\,X_2X_3[2] - 18.18\,X_2X_3[3] - 37.84X_1^2 \qquad (13)$$

Table 5. Estimated coefficients of the response models for ballistic properties

Response	Model terms	Coefficient	Standard error of coefficient	T-Value	p-value	R^2
Chamber pressure (P)	Constant	2.551E+005	5592.99	93.65	0.0001*	
	X_1	-50963.46	3063.41	276.76	0.0001*	
	X_2	23918.00	3063.41	60.16	0.0001*	
	$X_3[1]$	32523.31	4332.31	80.81	0.0001*	
	$X_3[2]$	87167.53	4332.31	80.81	0.0001*	
	$X_3[3]$	-29500.14	4332.31	80.81	0.0001*	
	X_1X_2	7704.00	3751.89	0.42	0.0527	0.9737
	$X_1X_3[1]$	31983.29	5305.98	24.19	0.0001*	
	$X_1X_3[2]$	-77906.87	5305.98	24.19	0.0001*	
	$X_1X_3[3]$	26635.63	5305.98	24.19	0.0001*	
	$X_2X_3[1]$	-10692.00	5305.98	3.07	0.0002*	
	$X_2X_3[2]$	29373.33	5305.98	3.07	0.0002*	
	$X_2X_3[3]$	-10457.83	5305.98	3.07	0.0002*	
	X_1^2	-20533.37	5305.98	14.98	0.0009*	
	X_2^2	-1122.00	5305.98	0.045	0.8346	
Chamber temperature (T)	Constant	1494.76	1.46	1566.86	0.0001*	
	X_1	-111.42	0.80	19305.43	0.0001*	
	X_2	33.07	0.80	1700.74	0.0001*	
	$X_3[1]$	6.66	1.13	60.41	0.0001*	
	$X_3[2]$	19.78	1.13	60.41	0.0001*	
	$X_3[3]$	-4.64	1.13	60.41	0.0001*	
	X_1X_2	8.04	0.98	67.08	0.0001*	
	$X_1X_3[1]$	1.82	1.39	19.41	0.0001*	0.9984
	$X_1X_3[2]$	-17.68	1.39	19.41	0.0001*	
	$X_1X_3[3]$	5.95	1.39	19.41	0.0001*	
	$X_2X_3[1]$	-1.47	1.39	1.61	0.0103*	
	$X_2X_3[2]$	5.28	1.39	1.61	0.0103*	
	$X_2X_3[3]$	-1.80	1.39	1.61	0.0103*	
	X_1^2	-15.21	1.39	119.96	0.0001*	
	X_2^2	-4.39	1.39	9.98	0.0047*	
Thrust (F)	Constant	461.59	9.94	96.68	0.0001*	
	X_1	-91.39	5.44	282.01	0.0001*	
	X_2	42.50	5.44	60.98	0.0001*	
	$X_3[1]$	57.32	7.70	80.88	0.0001*	
	$X_3[2]$	158.08	7.70	80.88	0.0001*	
	$X_3[3]$	-52.85	7.70	80.88	0.0001*	
	X_1X_2	15.04	6.67	5.09	0.0348	
	$X_1X_3[1]$	60.04	9.43	25.65	0.0001*	0.9745
	$X_1X_3[2]$	-141.58	9.43	25.65	0.0001*	
	$X_1X_3[3]$	47.40	9.43	25.65	0.0001*	
	$X_2X_3[1]$	-21.53	9.43	3.65	0.0002*	
	$X_2X_3[2]$	53.84	9.43	3.65	0.0002*	
	$X_2X_3[3]$	-18.18	9.43	3.65	0.0002*	
	X_1^2	-37.84	9.43	16.11	0.0006*	
	X_2^2	-2.76	9.43	0.086	0.7723	
Specific impulse (I_{sp})	Constant	82.92	1.53	58.93	0.0001*	
	X_1	-16.02	0.84	365.13	0.0001*	
	X_2	7.55	0.84	81.04	0.0001*	
	$X_3[1]$	-3.13	1.19	14.43	0.0001*	
	$X_3[2]$	12.42	1.19	14.43	0.0001*	
	$X_3[3]$	-0.40	1.19	14.43	0.0001*	
	X_1X_2	2.60	1.03	6.41	0.0194*	
	$X_1X_3[1]$	11.20	1.45	22.26	0.0001*	0.9589
	$X_1X_3[2]$	-19.65	1.45	22.26	0.0001*	
	$X_1X_3[3]$	7.03	1.45	22.26	0.0001*	
	$X_2X_3[1]$	-4.35	1.45	3.07	0.0004*	
	$X_2X_3[2]$	7.22	1.45	3.07	0.0004*	
	$X_2X_3[3]$	-2.58	1.45	3.07	0.0004*	
	X_1^2	-6.63	1.45	20.83	0.0002*	
	X_2^2	-0.31	1.45	0.047	0.8312	

* Significant at $p < 0.05$.

(a) Core
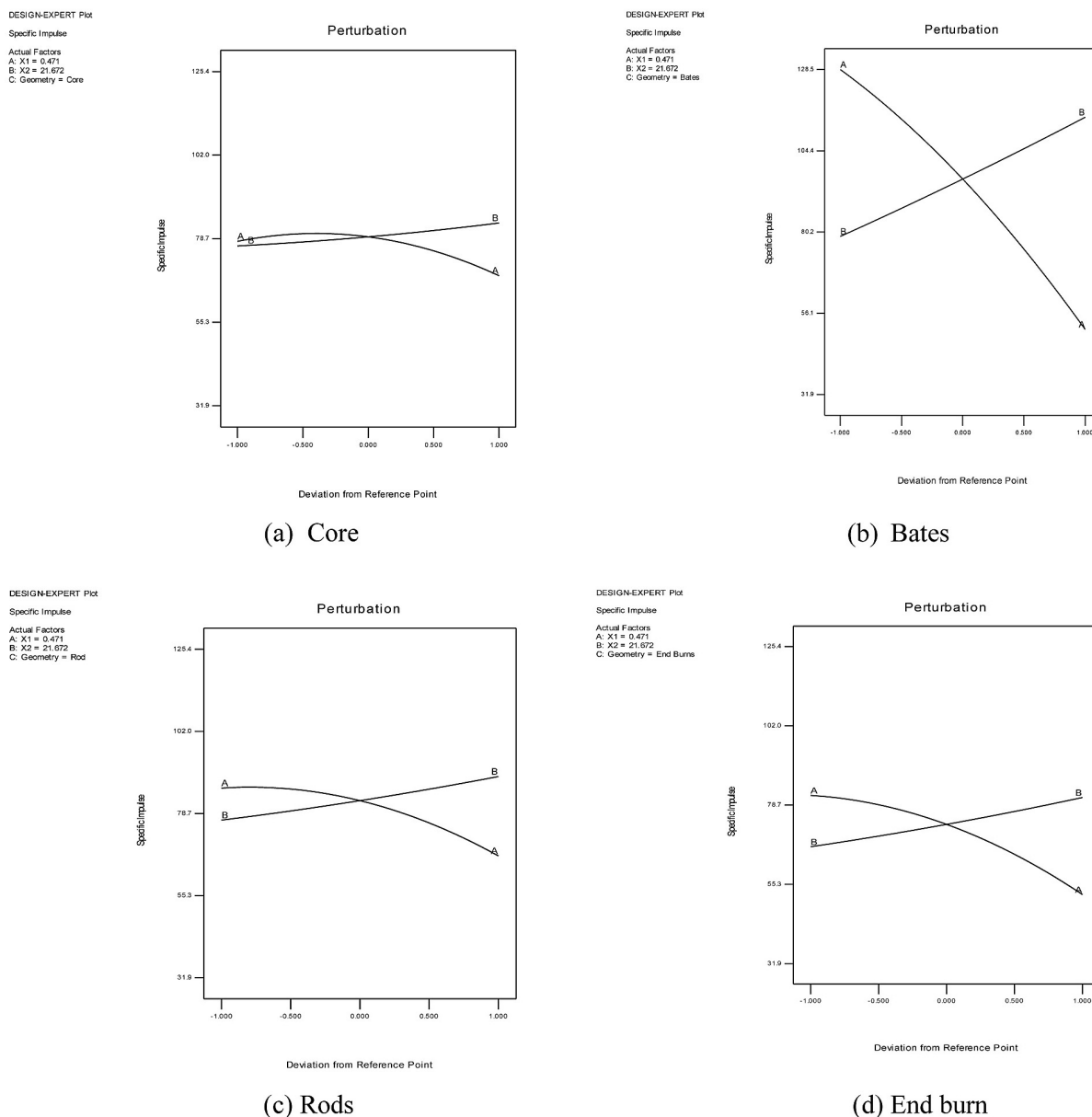

(b) Bates

(c) Rods

(d) End burn

Fig. 1. The effects of varying propellant compositions on the specific impulse for various grain geometries

$$I_{sp} = 82.92 - 16.02X_1 + 7.55X_2 - 3.13X_3[1] +$$
$$12.42X_3[2] - 0.40X_3[3] + 2.60X_1X_2 + \quad (13)$$
$$11.20X_1X_3[1] - 19.65X_1X_3[2] + 7.03X_1X_3[3] -$$
$$4.35X_2X_3[1] + 7.22X_2X_3[2] - 2.58X_2X_3[3] - 0.31X_1$$

As shown in the equations (11) – (14), most of the linear, quadratic and interaction terms of the models were significant. These models showed that the composition ratio and by implication the actual composition and the geometries all have effect on the final properties of the SRM internal system. The inclusion of sucrose, potassium nitrates and the geometry had various effects on the final performance of the SRM in terms of ballistic properties. In-

creasing the amount of sucrose in the composition reduces all the three properties while any increment in potassium nitrate increases their value. These fitted models were tested for adequacy and consistency using Analysis of Variance (ANOVA) and the values of various computation are as presented in Table 6.

The results from the ANOVA revealed that the F-values for chamber pressure, temperature, thrust and specific impulse are 675.03, 714.48, 694.02 and 592.74, respectively. These are significant at the 95% level. Also, using diagnostic plot of residual value against the actual value, there were no outlier in the plot and this confirms the stability of the model.

Table 6. Analysis of variance for fitted models for specific impulse

| Ballistic properties	Source of variation	Sum of squares	d.f.	Mean squares	F-values	Adjusted R^2
Chamber Pressure	Regression	2.95E^{+11}	14	1.52E^{+11}	675.03*	0.9737
	Residual	4.730E^{+9}	21	2.25E^{+8}		
	Total	3.000E^{+11}	35			
Temperature	Regression	338550.5	14	331009.7	714.48*	0.9984
	Residual	324.10	21	15.43		
	Total	3.389E^{+5}	35			
Thrust	Regression	962025.8	14	493284.7	694.02*	0.9745
	Residual	14926.05	21	710.76		
	Total	9.770E^{+5}	35			
Specific Impulse	Regression	14017.68	14	9994.90	592.74*	0.9589
	Residual	354.10	21	16.86		
	Total	14371.78	35			

* Significant level at $p < 0.05$.
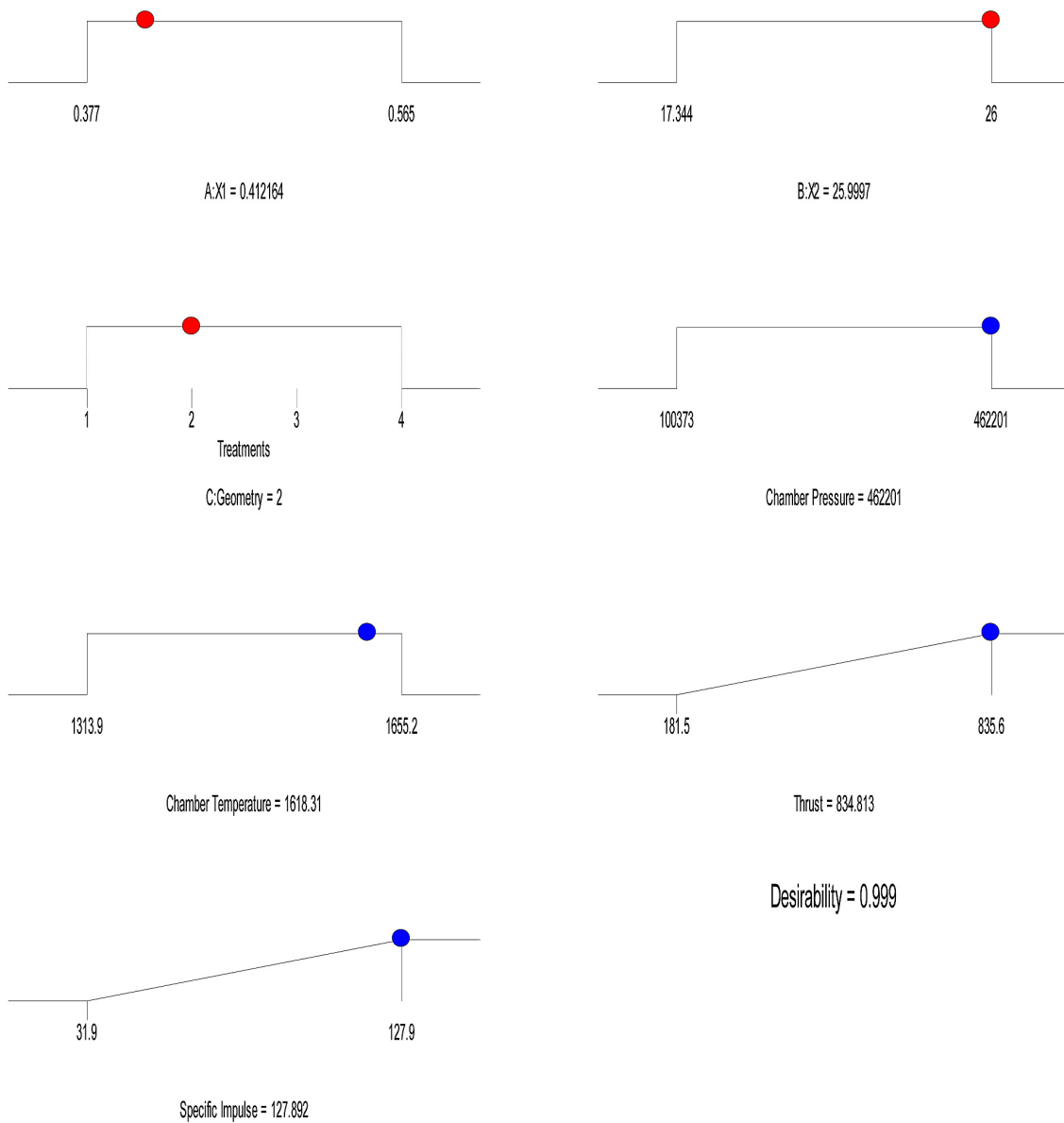
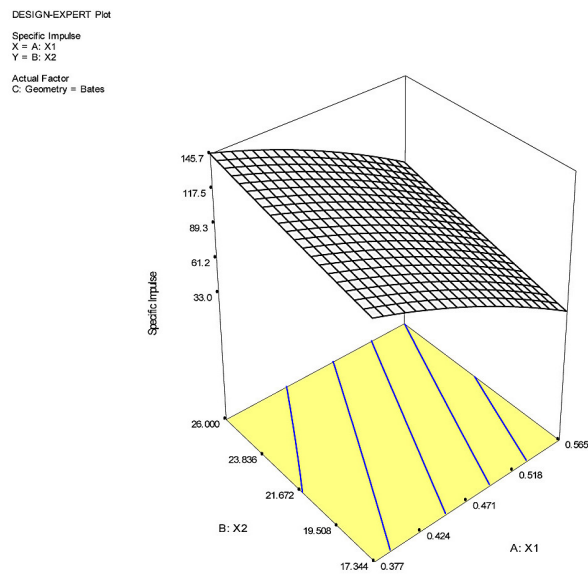**Fig. 2.** Optimization tree for propellant formulation
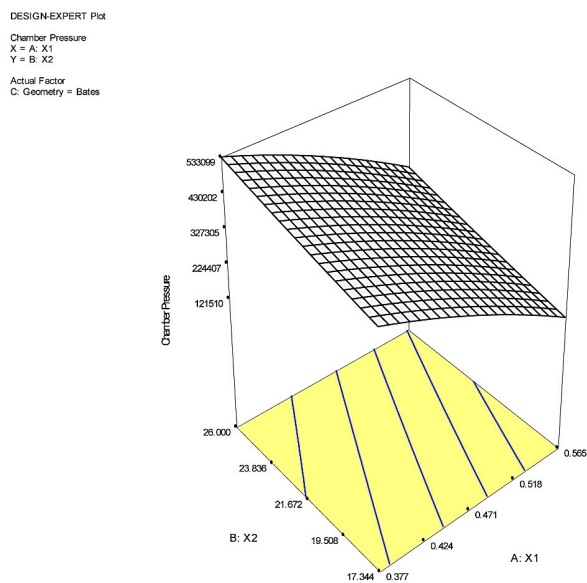
(a) Chamber pressure
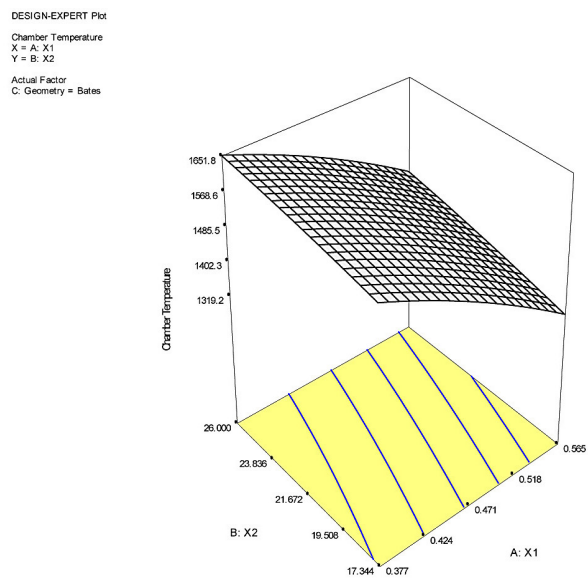
(b) Temperature
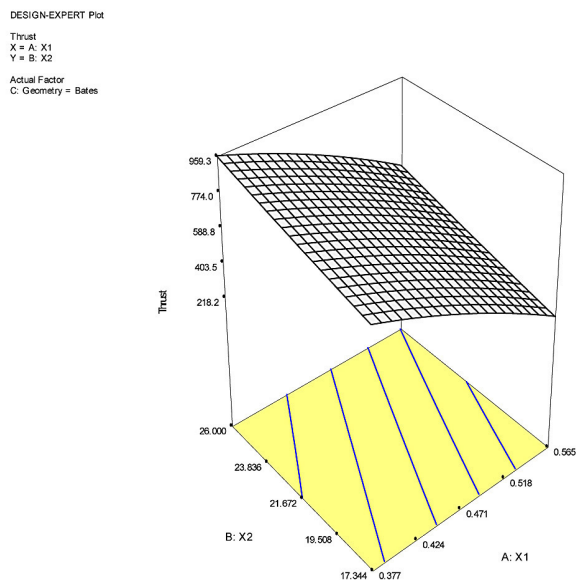
(c) Thrust

(d) Specific Impulse

Fig. 3. Response surface plots for optimum propellant composition

Optimization and validation of solid propellant formulation

The RSM was used to find the maximum specific impulse and thrust subject to the ranges of the chamber pressure and temperature. The optimum specific impulse obtained was 127.89 s, Chamber pressure (462201 Pa), Temperature (1618.31 K), Thrust (834.83 N) at sucrose ratio of 0.4122, potassium nitrate (25.9997) and bate geometry. As shown on the optimization tree Figure 2, the desirability index of the optimization procedure is 0.999 which is almost unity. This shows the level of optimality of the analysis. Another production constraints given was to minimize both the pressure and temperature while the thrust and specific impulse were maximized. The result of these two conditions were validated experimentally in triplicates and the average values of two set validations were compared with the optimum value using t-test. There were no significant difference between the validation and calculated values at $p < 0.05$. This affirms the reliability of the optimization framework developed. The actual weight

Table 7. Optimal propellant formulation

Categories	Variables	Optimization	
		Test 1	Test 2
Optimization Criteria for Calculation	Specific Impulse	Maximize	Maximize
	Thrust	Maximize	Maximize
	Pressure	Within range	Minimize
	Temperature	Within range	Minimize
Calculated Optimum Composition and Geometry	X_1	0.412	0.539
	X_2	26.000	26.000
	X_3	Bate (2)	Bate (2)
Calculated Optimum Composition In actual weight	A – Sucrose	0.584	0.700
	B – Potassium Nitrate	1.364	1.229
	C - Carbon	0.052	0.071
Calculated Optimum Level	Specific Impulse	127.89	82.40
	Thrust	834.83	535.78
	Pressure	462201	296007
	Temperature	1618.31	1452.96
Experimental Optimum Level	Specific Impulse	127.65 ± 0.89	83.10 ± 0.92
	Thrust	830.80 ± 1.84	528.90 ± 2.10
	Pressure	459897 ± 5.60	295982 ± 3.80
	Temperature	1630.2 ± 2.80	1440.60 ± 2.40
t - value		0.996*	2.052*

* Not significant at $p < 0.05$.

basis of the propellant formulation for the optimum mixes and their comparison are as shown on Table 7.

CONCLUSION

The ballistic properties increased with increase in potassium nitrate which is the oxidizer and decreased with increase in sucrose. and carbon. Therefore, potassium nitrate enhanced better specific impulse, which is the measure of propellant performance. Response Surface Methodology was successfully applied to the determination of the optimum formulation of solid propellant grains prepared using potassium nitrate and sucrose as main ingredient. The model predictions were accurate and reliable. Therefore, RSM is a reliable and powerful tool for optimization of solid propellant grains design and bate grain geometry is more efficient for minimizing the oscillatory pressure in the combustion chamber.

REFERENCES

1. Kamran A. and Guozhu L. An integrated approach for optimization of solid rocket motor. Aerospace Science and Technology, 17, 2012, 50–64.

2. Cai G., Hao Z., Dalin R., Hui T. Optimal design of hybrid rocket motor powered vehicle for suborbital flight. Aerospace Science and Technology, 25, 2013, 114–124.

3. Yumusak M. Analysis and design optimization of solid rocket motors in viscous flows. Computers and Fluids, 75, 2013, 22–34

4. Marimuthu R. and Rao B.N. Development of efficient finite elements for structural integrity analysis of solid rocket motor propellant grains. International Journal of Pressure Vessels and Piping, 112-113, 2013, 131–145.

5. DeLuca L., Galfetti L., Colombo G., Maggi F., Bandera A., Babuk V.A., Sinditskii V.P. Microstructure effects in aluminized solid rocket propellants. Journal of Propulsion and Power, 26 (4), 2010, 724–733.

6. Maggi F., Dossi S., DeLuca L.T. Combustion of metal agglomerates in a solid rocket core flow. Acta Astronautica, 92, 2013, 163–171.

7. Maggi F., Bandera A., Galfetti L., De Luca L.T., Jackson T.L. Efficient solid rocket propulsion for access to space. Acta Astronautica, 66 (11–12), 2010, 1563–1573.

8. Sutton G P. and Biblarz O. Rocket propulsion elements. John Wiley and Sons, 8th edition. New Jersey, 2010.

9. Yaman H., Celik V., Degirmenci E. Experimental investigation of the factors affecting the burning

rate of solid rocket propellants. Fuel, 115, 2014, 794–803.

10. Degirmenci E. Effects of grain size and temperature of double base solid propellants on Internal ballistics performance, Fuel, 146, 2015, 95–102

11. Turner M.J.L. Rocket and Spacecraft Propulsion: Principles, Practice and new Development, Third Edition. Praxis Publishing Ltd, Chichester, UK, 2009.

12. Kubato N. Propellant and explosives. Germany, 2002. ISBN: 3-527-30210-7.

13. Wu X.G., Yan Q.L., Guo X., Qi X.F., Li X.J., Wang K.Q. Combustion efficiency and pyrochemical properties of micron-sized metal particles as the components of modified double-base propellant. Acta Astronautica, 68, 2011, 1098–1112.

14. Meda L., Marra G., Galfetti L., Severini F., De Luca L. Nano-aluminum as energetic material for rocket propellants. Material Science and Engineering, 27, 2007, 1393–1396.

15. Song S.J., Kim H.J., Ko S.F., Oh H.T., Kim I.C., Yoo J.C., Jung J.Y. Measurement of solid propellant burning rates by analysis of ultrasonic full waveforms. Journal of Mechanical Science and Technology, 23, 2009, 1112–1117.

16. Peterson J., Garfield J. 1976, The automated design of multi-stage solid rocket vehicles, AIAA 76–744.

17. Walsh T., Wartburg R. Ballistic missile sizing and optimizing. AIAA 78-1019, 1978.

18. Sforzini R.H. An automated approach to design of solid rockets utilizing a special internal ballistic model. AIAA 80-1135, 1980.

19. Swaminathan V. and Madhavan N.S. A direct random search technique for the optimization of propellant systems. The Journal of the Aeronautical Society of India, 32, 1980, 23–32.

20. Truchot A. 1989, Overall optimization of solid rocket motors. AIAA 89-16916.

21. Fang Z. and Guo G. Optimization design of the solid rocket motor. Journal of Aerospace Power, 5, 1990, 176–178.

22. Guobiao C., Jie F., Xu X., Minghao L. Performance prediction and optimization for liquid rocket engine nozzle. Science and Technology, 11, 2007, 155–162.

23. Khurram N., Guozhu L., Qasim Z. A hybrid optimization approach for SMR Finocyl grain design. Chinese Journal of Aeronautics, 21 (6), 2008, 481–487.

24. Kamran A. and Guozhu L. Design and optimization of 3D radial slot grain configuration. Chinese Journal of Aeronautics 23, 2010, 409–414.

25. Kamran A. and Guozhu L. An integrated approach for optimization of solid rocket motor. Aerospace Science and Technology, 17, 2012, 50–64.

26. Yumusak M. and Eyi S. Design optimization of rocket nozzles in chemically reacting flows. International Journal of Computational Fluids, 65, 2012, 25–34.

27. Badyrka J.M., Hartfield R.J., Jenkins R.M. Aerospace design optimization using a compound repulsive particle swarm. Applied Mathematics and Computation, 219, 2013, 8311–8331.

28. Adami A., Mortazavi M., Nosratollahi M. A new approach in multidisciplinary design optimization of upper-stages using combined framework, Acta Astronautica, 114, 2015, 174–183.

29. Montgomery D.C. Design and analysis of experiments: Response surface method and designs. John Wiley and Sons, Inc., New Jersey, 2005.

30. Montgomery D.C. Water treatment principles and design. Wiley Interscience, New York, 2009, 175.

31. Richard A.N. Solid propellant rocket motor design and testing. An M.Sc thesis submitted to Faculty of Engineering, University of Manitobs, Manitobs, 1984, 133–145.

32. Robert A.B. Basics of space flight, rocket propulsion. A Wiley-Interscience Publication, New York City, 5th ed, 2009, 123–132.